Progressive vascular smooth muscle cell defects in a mouse model of Hutchinson–Gilford progeria syndrome

Renee Varga*, Maria Eriksson†, Michael R. Erdos*, Michelle Olive*, Ingrid Harten‡§, Frank Kolodgie¶, Brian C. Capell*, Jun Cheng‖, Dina Faddah*, Stacie Perkins*, Hedwig Avallone¶, Hong San*, Xuan Qu*, Santhi Ganesh*, Leslie B. Gordon*,**, Renu Virmani¶, Thomas N. Wight‡§, Elizabeth G. Nabel*††, and Francis S. Collins*‡‡

*Genome Technology Branch and ‖Genetic Disease Research Branch, National Human Genome Research Institute, National Institutes of Health, 50 South Drive, Bethesda, MD 20892; †Department of Medical Nutrition, Karolinska Institutet, Novum, Halsovagen 7, Hiss E, Plan 6, 141 57 Huddinge, Sweden; ‡Hope Heart Program, Benaroya Research Institute at Virginia Mason, Seattle, WA 98101-2795; §Department of Pathology, University of Washington School of Medicine, Seattle, WA 98195; ¶CVPath, Inc., 19 Firstfield Road, Gaithersburg, MD 20878; **Department of Pediatrics, Brown Medical School, Providence, RI 02912; and ††National Heart, Lung, and Blood Institute, National Institutes of Health, 31 Center Drive, Bethesda, MD 20892

Contributed by Francis S. Collins, January 2, 2006

Children with Hutchinson–Gilford progeria syndrome (HGPS) suffer from dramatic acceleration of some symptoms associated with normal aging, most notably cardiovascular disease that eventually leads to death from myocardial infarction and/or stroke usually in their second decade of life. For the vast majority of cases, a *de novo* point mutation in the lamin A (*LMNA*) gene is the cause of HGPS. This missense mutation creates a cryptic splice donor site that produces a mutant lamin A protein, termed "progerin," which carries a 50-aa deletion near its C terminus. We have created a mouse model for progeria by generating transgenics carrying a human bacterial artificial chromosome that harbors the common HGPS mutation. These mice develop progressive loss of vascular smooth muscle cells in the medial layer of large arteries, in a pattern very similar to that seen in children with HGPS. This mouse model should prove valuable for testing experimental therapies for this devastating disorder and for exploring cardiovascular disease in general.

lamin A | atherosclerosis | laminopathy

Children with Hutchinson–Gilford progeria syndrome (HGPS) appear normal at birth, but begin to display features of the disease postnatally (see Progeria Research Foundation's medical and research database at www.progeriaresearch.org). Progressive signs and symptoms include growth retardation, loss of hair, and s.c. fat, sclerodermatous skin, and bone abnormalities including craniofacial disproportion, mandibular, and clavicular hypoplasia, and osteoporosis (1). The most serious aspect of the disease, however, and the cause of death in >90% of cases, is rapid, progressive arterial occlusive disease, with death from myocardial infarction or stroke occurring at an average age of 13 years (range, 8–21 years).

Although autopsy data on progeria patients is very limited, consistent pathologic findings have been reported in the arterial system (2–5). Specifically, postmortem studies have identified profound loss of vascular smooth muscle cells (VSMC) in the medial layer of large arteries, such as the aorta and carotid arteries, with replacement by collagen and extracellular matrix. Superimposed on these medial changes have been generalized features of atherosclerosis with focal areas of calcification. The interlaminar spaces have been reported to contain thin and disorganized collagen fibrils as well as cell debris or matrix vesicles. Cholesterol clefts are lacking, and children with progeria have normal lipid profiles.

HGPS is caused in nearly all classic cases by a *de novo* mutation, 1824C→T (also denoted as G608G; i.e., the encoded amino acid for codon 608 remains glycine), in exon 11 of the lamin A/C gene on chromosome 1 (6, 7). Some atypical cases of progeria and Werner's syndrome have also been traced to other mutations in the *LMNA* gene (6, 8–12). There are at least eight other diseases in addition to HGPS caused by *LMNA* mutations, collectively known as the "laminopathies" (13). These include Dunnigan-type familial partial lipodystrophy, mandibuloacral dysplasia, Charcot–Marie–Tooth disorder-type 2, dilated cardiomyopathy-type 1A, and Emery–Dreifuss muscular dystrophy. Currently, over 180 *LMNA* mutations have been found in connection with these various laminopathies.

The three normal protein products of the *LMNA* gene, lamin A, lamin C, and lamin AΔ10, are all components of the nuclear lamina (14). The nuclear lamina is located just under the inner nuclear membrane and plays significant roles in nuclear shape, DNA replication and transcription, cell division, and chromatin organization. Lamin A is posttranscriptionally modified. The initial precursor, prelamin A, undergoes a series of processing steps that include farnesylation of the cysteine in the C-terminal CAAX sequence, cleavage of the terminal AAX sequence with addition of a methoxy group to the terminal cysteine, and subsequent cleavage of the terminal 15 aa by the protease ZMPSTE24. The HGPS mutation in exon 11 creates a novel splice donor site 150-bp upstream of the true exon 11 splice donor site. The protein that is encoded by using the cryptic splice site, which we call progerin, lacks 50 aa near the C terminus. Within these 50 aa is the ZMPSTE24 recognition site. Progerin is thus unable to be cleaved, resulting in a permanently farnesylated form of lamin A (6, 15). We hypothesized that the retention of the farnesyl group forces progerin to remain embedded in the nuclear membrane and form multimeric complexes with mature wild-type lamin A and other proteins, creating a mislocalized multiprotein complex that alters nuclear structure and function. In support of this hypothesis, mutations in ZMPSTE24 cause a severe form of mandibuloacral dysplasia, which is phenotypically similar to HGPS (16).

Several useful mutant *Lmna* mouse models have been created and studied (17–19). Functional knockout of the *Lmna* gene in mice produces a cardiac and skeletal myopathic phenotype similar to human Emery–Dreifuss muscular dystrophy (17). Mounkes *et al.* (18) also reported a knock-in of the L530P mutation, associated in humans with autosomal dominant Emery–Dreifuss muscular dystrophy. Heterozygous $Lmna^{L530P/wt}$ mice are indistinguishable from wild-type (WT) mice, but homozygous mice have a phenotype resembling HGPS, with severe growth retardation within 4–5 days and death within 4–5 weeks. Features that these mice share with children with HGPS include micrognathia and abnormal dentition,

Conflict of interest statement: No conflicts declared.

Abbreviations: HGPS, Hutchinson–Gilford progeria syndrome; VSMC, vascular smooth muscle cells; WT, wild type; BAC, bacterial artificial chromosome; PG, proteoglycan; NP, sodium nitroprusside.

‡‡To whom correspondence should be addressed at: National Human Genome Research Institute, National Institutes of Health, Building 31, Room 4B09, 31 Center Drive, MSC2152, Bethesda, MD 20892-2152. E-mail: fc23a@nih.gov.

www.pnas.org/cgi/doi/10.1073/pnas.0600012103

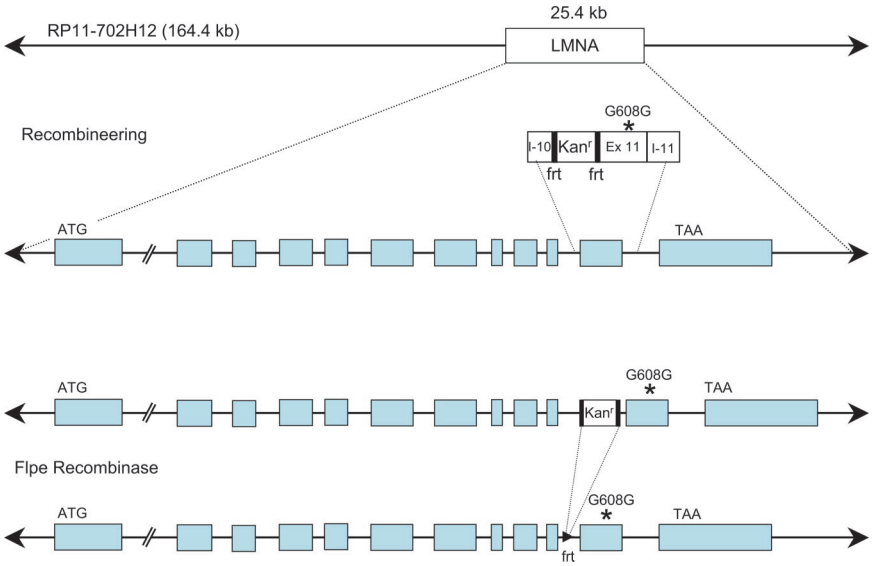

Fig. 1. Procedure for generating the BAC G608G transgenic construct by homologous recombination in *E. coli*. Human BAC clone RP11-702H12 contains an insert of 164.4 kb of genomic DNA from chromosome 1q including the *LMNA* gene. Homologous recombination was induced between this BAC and a shuttle fragment of 2.3 kb containing the common G608G HGPS mutation within exon 11 (Ex 11) of *LMNA* and the kanamycin resistance gene (*Kan*^{r}) flanked by two FRT sites. Homology arms with sequences from intron 10 (I-10) and intron 11 (I-11) of the *LMNA* gene were used to direct the recombination event between the shuttle fragment and the BAC clone. After selection for positive recombinants, Flpe recombinase was induced to release the kanamycin gene. The final BAC G608G transgenic construct used for pronuclear injection differs from the original BAC in that it contains the G608G mutation (*) within exon 11 of *LMNA* and 109 extra nucleotides in intron 10 including an FRT site, EcoRI site, and SacI site.

absence of the s.c. fat layer, sclerodermal-like increases in collagen, decreased bone density, malformation of the scapulae, and hypogonadism. Nevertheless, these mice have no obvious defects in the aorta or large vessels (18), and recent studies have documented that the knock-in allele actually causes a more complex splicing anomaly. Yang *et al.* (19) have recently reported a knock-in model whose mutant *Lmna* allele codes exclusively for progerin, without any normal lamin A or C. Heterozygotes exhibit growth retardation and bone disease, but detailed phenotypic characterization of the vascular system has not yet been reported for these animals.

We created a transgenic mouse that carries the G608G mutated human *LMNA* on a 164-kb bacterial artificial chromosome (BAC). Although this mouse lacks the external phenotype seen in human progeria, it does demonstrate the progressive vascular abnormalities that closely resemble the most lethal aspect of the human phenotype.

Results

Using a two-step recombination protocol in *Escherichia coli* (20), we modified a human BAC containing the *LMNA* gene to carry the HGPS G608G mutation (Fig. 1). G608G transgenic mice were created by injecting BAC DNA, both as a circular construct and after linearizing with a unique PI-SceI restriction site. As a control, transgenics were also produced carrying a WT *LMNA* BAC. Sixteen founders who carry the transgene as determined by PCR analysis were born and bred for the G608G constructs, eight from the circular and eight from the linearized BAC. Founders F, G, and H of the eight circular G608G BAC founders expressed progerin. Offspring of founder H were used for the majority of studies reported here. Of the eight linearized G608G BAC founders, founders C, D, and H expressed progerin. For the WT BAC transgenics, the circular construct produced five founders. Only founder B expressed the transgene, and therefore, that line was expanded. Of the three founders for the linearized WT BAC construct, founder A expressed the transgene, and that line was expanded. Southern blotting suggested a single copy of the BAC in the G608G H-line, WT transgenic B-line, and WT transgenic A-line mice (data not shown).

Consistent vascular pathologic changes were found in founders F and H from the circular G608G BAC construct and founder C from the linearized G608G BAC (see below). Founder B from the circular WT BAC and founder A from the linearized WT BAC showed no pathologic changes in any tissue, except for possibly very mild fragmentation of elastin and occasional small foci of proteoglycan (PG) deposition in the medial layer of large vessels at advanced age.

RT-PCR and Western blotting indicated that the *LMNA* transgene and the lamin A, lamin C, and progerin proteins were being expressed in all tissues tested (bone, ear, skin, brain, heart, aorta,

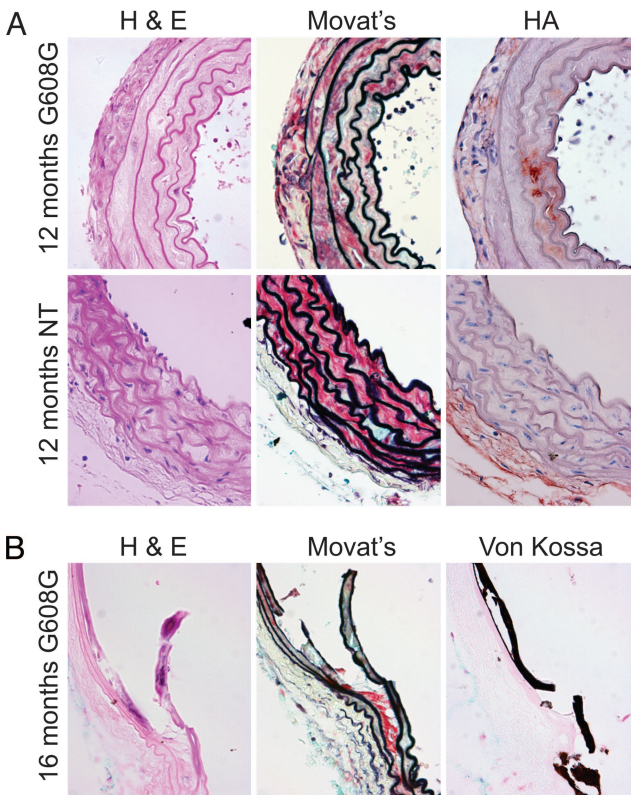

Fig. 2. Progressive arterial abnormalities in progeria mice. (*A*) Analysis of aortic sections of 12-month-old mice by using hematoxylin/eosin (H & E) and Movat's pentachrome stain and immunohistochemistry analysis for hyaluronan indicates a progressive loss of VSMC, elastin breakage, thickened medial layer and adventitia, and PG accumulation. (*B*) All G608G mice examined over 16 months of age showed evidence of carotid (shown) and aortic (data not shown) calcification, which was confirmed with Von Kossa staining. Younger HGPS and all ages of NT mice showed no evidence of calcification. HA, hyaluronan.

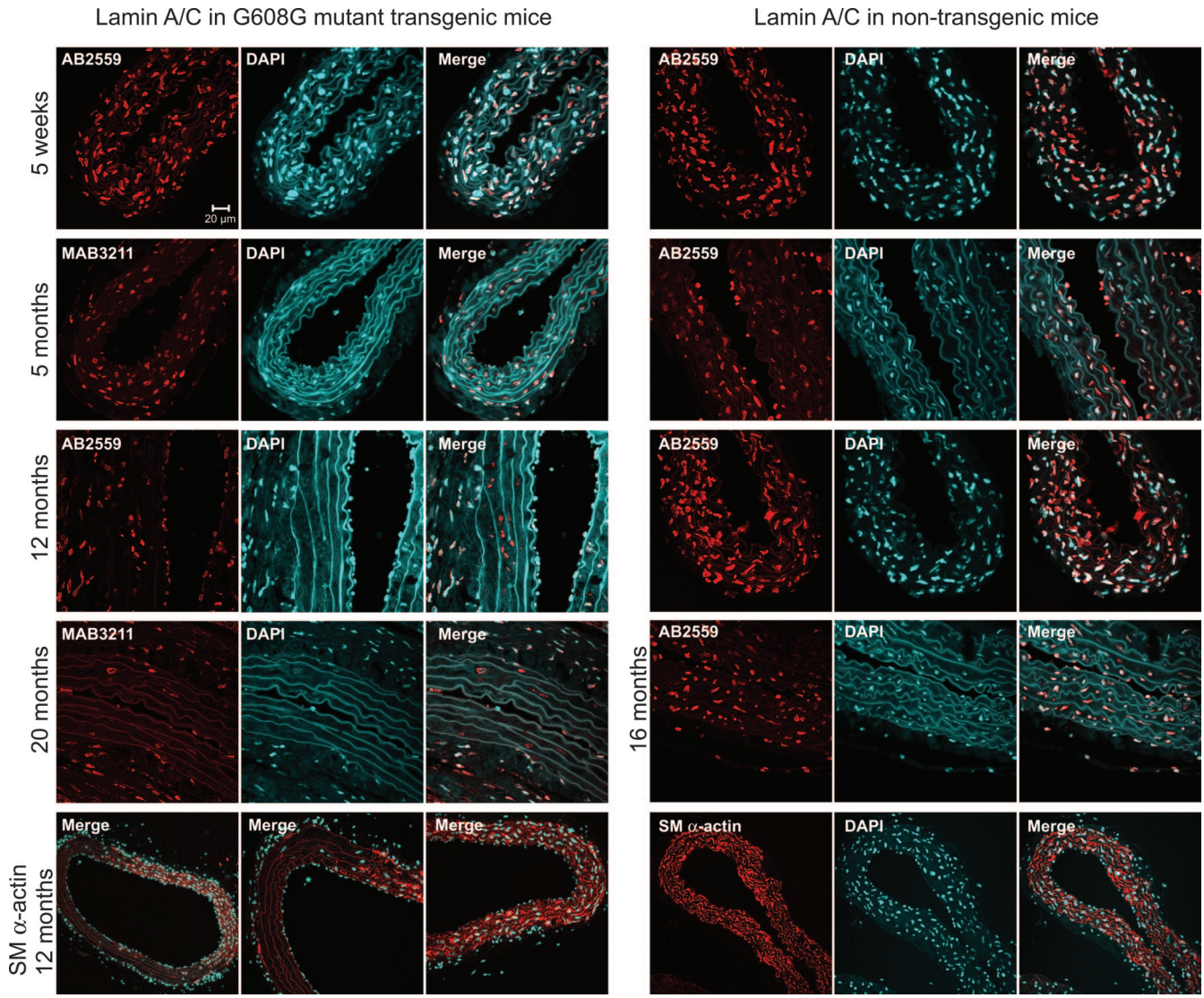

Fig. 3. Lamin A immunofluorescent staining of aortic sections highlights the progressive VSMC loss in G608G transgenics. The presence of lamin A/C is detected in descending aorta by using either the mAb3211 antibody (detects human but not mouse) or the Ab2559 antibody (detects both human and mouse). The age of each animal is indicated on the figure. The nuclei are counterstained with DAPI (blue), and an overlay of the lamin A/C and DAPI images is presented (merge). Cells with lamin A/C staining are present in the three layers of the arteries: intima, media, and adventitia in 5-week-old and 5-month-old transgenic mice. The number of lamin A/C-positive nuclei is dramatically decreased in the 12-month-old mice. They are almost completely absent in the medial layer of older transgenic animals (20 months). Note the presence of ''ghost'' nuclei in the 12- and 20-month-old G608G mice that retain lamin A/C staining, but lack DAPI staining. Smooth muscle α-actin staining confirms loss of VSMCs; these images also show the eccentric distribution of vascular damage, with some areas around the vessel circumference better preserved than others.

carotid artery, iliac artery, skeletal muscle, liver, kidney, spleen, testis, and ovary) for the G608G H-line, G608G founder C-line, and WT transgenic A-line and B-line mice (see Fig. 6, which is published as supporting information on the PNAS web site, and data not shown). No consistent differences in mortality, size, hair loss, teeth, or skin quality were seen between the G608G H-line mice and the WT transgenic and nontransgenic mice $\leq$20 months of age.

Tissues were surveyed at autopsy and by microscopic analysis. No consistent pathology was found in the external ear, skin, brain, testis, ovary, skeletal muscle, bone, liver, spleen, kidney, or heart for the G608G H-line mice. Sections of aorta, carotid artery, and iliac artery were stained with hematoxylin/eosin and Movat's pentachrome stains. In the G608G mice, the most dramatic finding was the progressive loss of VSMC, elastic fiber breakage, thickening of the adventitia and medial layer, accumulation of PGs, and collagen deposition. This phenomenon was first observed in 5-month-old mice and became severe by 12 months. Arterial calcification was observed in older mice with severe VSMC loss and extracellular matrix deposition. No inflammation was present, and the VSMC that remained appeared hypertrophied. Although all large arteries screened were abnormal, the descending aorta (Fig. 2*A*) and carotid artery were the most severe. Affinity histochemistry confirmed an accumulation of hyaluronan with age, which was absent in controls (Fig. 2*A*). Von Kossa staining confirmed the progressive calcification found in vessels from older G608G mice; such calcium deposits were absent in age matched controls (Fig. 2*B*).

To visualize expression of the transgene in microscopic sections, we took advantage of the fact that the lamin A/C antibody (Ab2559) recognizes both human and mouse lamin, but the lamin A monoclonal antibody (mAb3211) recognizes human lamin A and not mouse lamin A. Immunohistochemistry using these antibodies showed that in 5-week-old G608G and the controls lamin A/C was

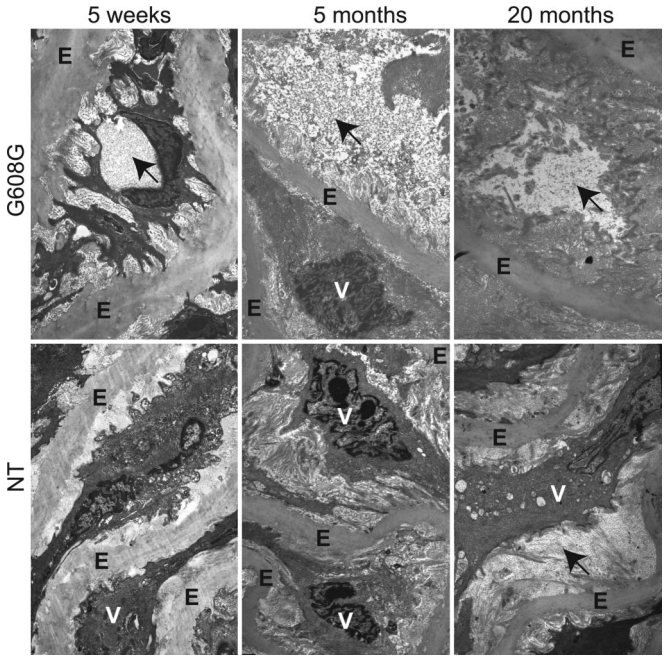

Fig. 4. Transmission electron microscopy comparing nontransgenic (NT) and G608G H-line carotid artery sections showing in the G608G line the progressive accumulation of cellular debris, frayed elastin fibers, and accumulation and disorganization of collagen and PG (see black arrows). The nontransgenic vessel shows only mild changes at 20 months. E, elastin; V, VSMC.

present in the endothelial cells, in the medial VSMC, and in the adventitia. Over the next 6–12 months, progressive loss of VSMC was observed in G608G transgenics in an eccentric pattern around the vessel circumference. As the mice reached a more advanced age (20 months), complete depletion of the medial VSMC occurred in many regions (Fig. 3). Similar observations were made in the carotid artery (see Fig. 7, which is published as supporting information on the PNAS web site). We also noticed the presence in older animals of protein debris nuclear "ghosts" that are positive for lamin A but lack DNA (Fig. 3 and see Fig. 8, which is published as supporting information on the PNAS web site). Smooth muscle α-actin staining confirmed the eccentric VSMC loss in the medial layer of large arteries, whereas the endothelial cells remained essentially intact (Fig. 3 and see Fig. 7).

Transmission electron microscopy analysis of descending aorta and carotid showed cellular debris, apparently derived from the remnants of disintegrating VSMC. An abnormal extracellular matrix was also visible, with accumulated PG, highly disorganized collagen fibrils, and frayed elastic fibers displaying variable thickness (Fig. 4).

The status of cell proliferation in the carotid artery and descending aorta was investigated by BrdUrd analysis on three mice from each age group (5 weeks, 5 months, and 14+ months) in the G608G H-line and control mice. Although the control tissue (thymus) stained positive for proliferating cells, no cells were proliferating in the vessel medial layer of transgenic and control mice (data not shown). TUNEL staining of sections to look for evidence of apoptosis was inconclusive.

In smooth muscle α-actin knockout mice, blood pressure in response to the vasodilator, sodium nitroprusside (NP), was observed to be blunted (21). We, therefore, hypothesized that the loss of VSMC in our transgenic mice would similarly lead to abnormal arterial response to NP administration. Blood pressure was measured before and after NP infusion for G608G and nontransgenic mice. Mice were studied at 5 weeks and 5 months of age. At 5 weeks, average baseline mean arterial pressure and blood pressure lowering by NP was equivalent in the two groups. At 5 months of age, baseline blood pressure tended to be slightly lower in the G608G transgenics than the controls, but this difference was not significant. After infusion of NP, blood pressure lowering in 5-month-old mice was significantly blunted in the G608G group, as measured by the difference in mean arterial pressure before and after infusion ($P = 0.02$, one-tailed t test). Values obtained at 5 months for the difference in mean arterial pressure before and after infusion are 41, 38, and 40 mmHg (1 mmHg = 133 Pa) for the nontransgenic mice and 34 and 27 mmHg for the G608G mice. Additionally, impaired recovery of blood pressure to baseline levels was observed for several minutes after infusion in transgenic animals (Fig. 5).

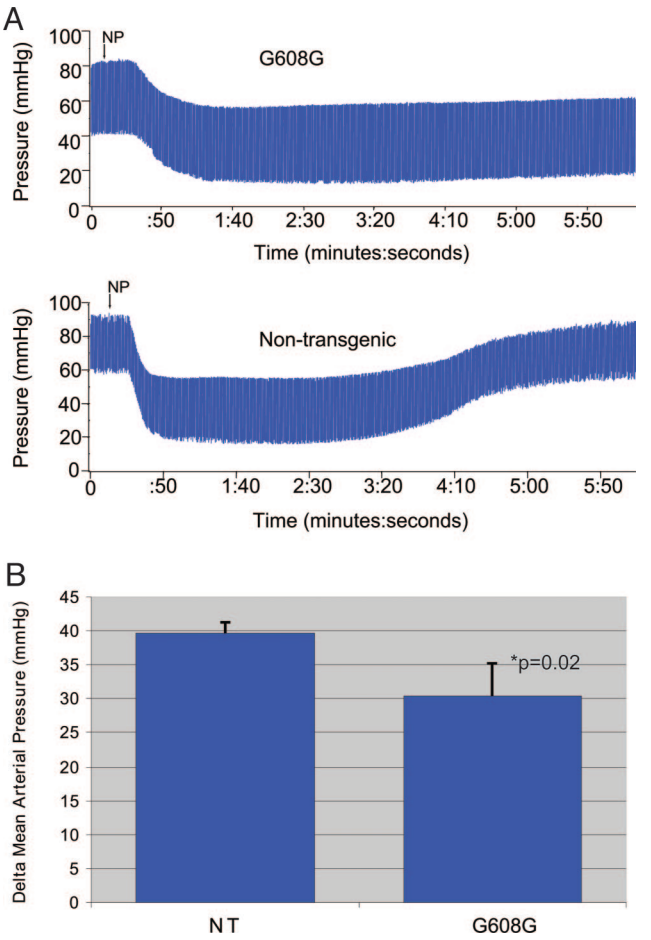

Fig. 5. Diminished vascular responsiveness in progeria mice. (*A*) Representative blood pressure tracings taken before and after NP administration in 5-month-old mice. (*B*) The drop in mean arterial pressure, comparing blood pressure before and after the administration of NP, is blunted in the G608G mice as compared with the control mice at 5 months of age.

Discussion

To further the understanding of the pathogenesis of HGPS, we created a mouse model by using the human *LMNA* gene containing the G608G mutation. A knock-in might have initially seemed like a more direct approach, but we were concerned that introducing this single nucleotide change into the mouse *Lmna* gene might or might not result in similar activation of a splice donor and production of mouse progerin. Therefore, it seemed more prudent to introduce the human G608G *LMNA* gene. We chose to use a human BAC containing the *LMNA* gene and substantial flanking DNA to include regulatory signals and obtain a faithful developmental pattern of expression.

GENETICS

There were risks associated with this strategy. Creating an extra copy of *LMNA* could cause a phenotype of its own. Regulation of the human BAC transgene might be different in the murine environment. Furthermore, the 164-kb BAC carries other genes (*UBQLN4, MAPBPIP*, and *RAB25*) in addition to *LMNA*, which could also affect the phenotype. All of these concerns were addressed by creating control animals carrying a WT human *LMNA* BAC. The phenotype of the WT transgenics was essentially normal, except for possibly very mild medial arterial changes in animals of advanced age, although this was difficult to distinguish from nontransgenic controls.

G608G transgenic mice were found to have a progressive and dramatic defect of the large arteries, consisting of progressive medial VSMC loss and replacement with PG and collagen. In addition, the arteries underwent vascular remodeling in response to the VSMC loss, with calcification and adventitial thickening. We were unable to determine whether VSMC were undergoing apoptosis or replicating to replace their loss because cell turnover was too slow to detect with BrdUrd or TUNEL staining. These arterial abnormalities were reflected functionally by an altered *in vivo* response to the vasodilator NP. G608G mice demonstrated a blunted initial response to NP, consistent with impaired vascular relaxation and attenuated blood pressure recovery after infusion.

Although G608G transgenic mice lack pathologic features of HGPS outside of the vascular system, the pathologic changes in the medial layer of large vessels show pronounced similarity to the human condition (2–5). Both human progeria patients and the G608G transgenic mice have severe VSMC loss, accumulation of acellular material, and calcification of the vessel wall. The pattern in human progeria also includes some degree of intimal proliferation, which is also a form of vascular remodeling, probably in response to the progressive loss of medial VSMC (2–5). We observed minimal intimal thickening in the transgenic mice; however, it is possible that intimal thickening would occur in response to vascular injury or other cardiovascular insults.

LMNA and progerin are expressed in a variety of tissues in these transgenic animals. Why, then, is the mouse phenotype essentially limited to VSMC in large arteries? Based on the report of Lammerding *et al.* (22) that lamin A/C-deficient mouse embryo fibroblasts are more sensitive to mechanical strain, we propose that progerin-expressing VSMC in the aorta and proximal arterial tree are in particularly vulnerable locations to experience mechanical stress. Thus, the shear forces from blood forcefully pounding against arterial walls, particularly in the aortic arch and at bifurcations, progressively devitalizes VSMC that have been rendered unusually fragile by the presence of progerin, ultimately leading to an almost acellular vessel wall. Perhaps, other tissues would show effects if the mice lived longer.

This model will potentially be useful to further the understanding of the underlying cause of the vascular pathology in progeria and to study potential therapies. For example, we and others recently reported that the use of farnesyltransferase inhibitors can improve the abnormal nuclear structure of human progeria fibroblasts *in vitro* by correcting the blebbing that is a hallmark of the disorder (15, 23–25). Additionally, bone marrow transplantation from a compatible normal donor might provide stem cells that could repopulate the depleted arterial medial layer in HGPS. A similar strategy has been reported to improve the clinical status of children with osteogenesis imperfecta (26). Both drug therapy and transplant approaches to progeria can now be tested with this mouse model.

Materials and Methods

Generation of *LMNA* G608G Transgenic Mice. The human BAC clone, RP11-702H12 (RPCI-11 Human BAC Library, BACPAC Resource Center at Children's Hospital Oakland Research Institute, Oakland, CA) contains an insert of 164.4 kb of genomic DNA from chromosome 1q including the *LMNA* gene (25.4 kb) and three other known genes, *UBQLN4*, *MAPBPIP*, and *RAB25*. Recombinogenic targeting of BAC clone RP11-702H12 was performed with a shuttle fragment containing the G608G mutation, surrounding upstream and downstream elements of the *LMNA* gene, and the *kan*^{r} gene flanked by FRT sites. The shuttle fragment was constructed by PCR amplification of genomic DNA from HGPS sample AG11498 [carrying G608G (6)] with primers: NotI-AACAGGGAACCCAGGTGTCT and EcoRI-AGGAAAAATGAGGGAAATGAGAG, SacI-GCAAGAATGTTCTCTCTCATTCC and SalI-CAGGATTTGGAGACAAAGCAG; and by PCR amplification of vector pIGCN21 with primers: EcoR1-CGGGATCCACCGGATCTA and SacI-TGGAGGCTACCATGGAGAAG. Following PCR amplification, the fragments were purified, digested, and ligated to pBluescript II KS(+) (Stratagene). Before recombineering, the shuttle fragment of 2.3 kb was released from its carrier by digests with NotI and SalI and then was gel-purified. Recombineering was performed in the recombinogenic bacterial strain EL250 in accordance with procedures described in refs. 20 and 27, and *kan*^{r} clones were screened by PCR for integration of the shuttle fragment by using primers: GTAGACATGCTGTACAACCC and SacI-TGGAGGCTACCATGGAGAAG. Following identification of positive clones, FLP recombination was induced to remove the kanamycin resistance gene (20). PCR of the different *LMNA* exons, sequencing of the region targeted for recombination, and fingerprinting of BAC clone digests with HindIII and XbaI from different steps in the recombination process confirmed removal of the kanamycin resistance gene and showed no additional recombination in the final clone used for the production of the transgene. Double CsCl banding (Lofstrand Laboratories, Gaithersburg, MD) was used to purify the BAC clones before injection into the male pronucleus of recently fertilized C57BL/6 embryos. Unmodified purified RP11-702H12 was also injected for use as a control. Injections with circular and linearized BAC clones were performed for each of the BAC clones (RP11-702H12 G608G and RP11-702H12 unmodified). For linearized injections, the CsCl-purified BAC DNA was digested with PI-SceI, which cuts once in the vector, before injection. All animal use complied with the Animal Care and Use Committee guidelines (National Institutes of Health, Bethesda).

Mouse Genotyping. DNA was extracted from tail biopsies according to standard phenol-chloroform methods. Genotyping was performed on genomic DNA by PCR analysis by using primers to amplify a fragment in intron 10 (5′-AACAGGGAACCCAGGTGTCT-3′ and 5′-GCAGCAGGCATGCACTATTA-3′). The PCR product for the G608G transgene is 545-bp long. The PCR product for the WT transgene is 436-bp long. Southern blotting was also performed according to standard methods by using EcoRI to digest genomic DNA and taking advantage of an EcoRI site that is introduced into exon 10 in the G608G transgene. The probe was created by digesting a minigene construct that consists of a modified lamin A cDNA to include intron 11 with BamHI and HindIII. The 1372-bp fragment that includes exons 6–11, intron 11, and exon 12 was cut from the 1% TAE gel and purified by using Gene Clean (Qbiogene, Irvine, CA). The probe hybridizes to exon 11, intron 11, and exon 12 of an EcoRI-digested genomic fragment of 6673 bp and a fragment of 9707 bp for hybridization to exons 6–10 from G608G transgenic mice. Transgenic mice for the WT BAC were predicted to have a hybridization band of 16,378 bp, and the probe binds a 10,406-bp fragment from endogenous mouse DNA.

Transgene Expression Analysis. RNA was extracted from homogenized mouse tissues by using either TRIzol (Invitrogen) or the Fast RNA Pro Green kit (Qbiogene). Reverse transcription was performed by using Invitrogen's SuperScript II RT-PCR kit. PCR of the cDNA was performed by using primers 5′-GCAACAAGTCCAATGAGGACCA-3′ and 5′-GTCCCAGATTACATGATGC-3′. The PCR products produced include mouse lamin A (643 bp), human lamin A (640 bp), and progerin (490 bp). To differentiate

between endogenous mouse and transgenic human lamin A, BstUI was used to digest RT-PCR products, resulting in two bands for human (386 and 254 bp) and one band for mouse (643 bp). Protein extracted by using a radioimmunoprecipitation assay was run on 8% Tris/glycine gels (Invitrogen) and probed with mAb3211 lamin A antibody (Chemicon International) and goat anti-mouse horseradish peroxidase secondary antibody (Kirkegaard & Perry Laboratories). Visualization of the bands was possible by using the ECL-plus kit (Amersham Pharmacia Biosciences) and then developing the images on film (Kodak).

Histochemistry. Tissues fixed in 2% paraformaldehyde were dehydrated with graded alcohols and embedded in paraffin. Cross-sections (4-μm thick) were cut with a rotary microtome and mounted on charged slides (Superfrost, Columbia Diagnostics, Springfield, VA) and then stained with hematoxylin/eosin and Movat's pentachrome stain (28, 29). Images were captured by using an Olympus BX51 Microscope equipped with an Olympus DP11 digital camera. Images were managed by using Microsoft DIGITAL IMAGE PRO 10 and Adobe PHOTOSHOP 7 for WINDOWS.

Immunohistochemistry. Staining for lamins was performed in PBS by using the rabbit polyclonal anti-lamin A diluted 1:10 (Ab2559, Abcam, Inc., Cambridge, MA) on transgenic or nontransgenic tissues or the mouse monoclonal anti-lamin A/C nondiluted (mAb3211, Chemicon) on transgenic tissues with goat anti-rabbit or goat anti-mouse Alexa Fluor 594-conjugated secondary antibodies (Molecular Probes). Antigen retrieval was performed before the incubation of the lamin antibodies and consisted of a 2-min incubation in EDTA (0.37 g/liter) in a pressure cooker. A mouse-to-mouse blocking kit (ScyTek Laboratories, Logan, Utah) was used with mouse anti-lamin A/C. Staining for smooth muscle α-actin was performed by using a Cy3-conjugated antibody diluted 1:100 (Sigma–Aldrich). Slides were mounted in DAPI-containing medium (Vector Laboratories) Fluorescence emission images were obtained with a confocal microscope system (Zeiss LMS 510) and collected with $\times$20 or $\times$40 oil lenses (Zeiss).

PGs were detected in paraffin sections of vessels, after digestion with 0.2 units/ml chondroitin ABC lyase (Seikagaku America, Rockville, MD) for 1 h at 37°C, by using rabbit anti-mouse monoclonal antibodies (a gift from Larry Fisher, National Institute of Dental and Craniofacial Research, National Institutes of Health, Bethesda) against versican (LF99), biglycan (LF106), and decorin (LF113) and by using a rat anti-mouse monoclonal antibody against perlecan (a gift from Koji Kimata, Nagoya University, Chikusa, Nagoya, Japan). Biotinylated secondary antibodies were used (Vector Laboratories) and visualized by using Vector Red reagent (Vector Laboratories). Hyaluronan localization was carried out with a commonly used biotinylated probe consisting of a mixture of cartilage, PG, and link protein (provided by T.N.W.).

For BrdUrd analysis, the mice were given 100 mg/kg BrdUrd (Sigma) via i.p. injection 18 and 1 h before death. Sections of aorta, carotid, and thymus were prepared as discussed in ref. 29. Quantification of proliferating cells was performed by three blinded observers counting the number of BrdUrd-positive medial VSMC. Systemic distribution of BrdUrd was confirmed by intense staining of proliferating thymus cells in all animals receiving the agent.

Transmission Electron Microscopy. Samples were prepared and viewed by using a JEM 1200EX II transmission electron microscope (JEOL) as described in ref. 30. Images were acquired and saved on Kodak 4489 electron microscope film with a "below the viewing screen" film transfer system and scanned at 600 dots per inch by using an Epson Expression 1680 flat bed scanner for digitization. Ruthenium Red was used in some samples to gain better visualization of PGs.

Blood Pressure Analysis. Blood pressure was measured invasively by using a microtip pressure transducer catheter connected to an electrostatic chart recorder (Millar Instruments, Houston). Animals were anesthetized with 1–3% isoflurane, and the right external carotid artery was cannulated. Once initial baseline blood pressure measurements were completed, the mouse was infused with saline (30 μl over 2 min), and blood pressure was again measured. Sodium nitroprusside (1.5 mg/kg of body weight, 30 μl of total volume over 2 min) was then infused, and blood pressure measurements were taken until a return to baseline or a maximum of 20 min. For 5-week-old mice, three G608G and three nontransgenic mice were studied. For 5-month-old mice, two G608G and three nontransgenics were included. Because we postulated that the G608G animals would have a blunted response to NP, we used a one-tailed type-2 *t* test to assess significance, and this was performed by using Microsoft EXCEL.

We thank Darryl Leja for assistance in preparing the figures, Drs. David Bodine and Shelley Hoogstraten-Miller for mouse expertise, Dr. Christian A. Combs and Daniela Malide [Light Microscopy Core Facility, National Heart, Lung and Blood Institute, National Institutes of Heath (NIH)] for assistance regarding microscopy-related experiments, and Shih Queen Lee-Lin for DNA fingerprinting of BAC constructs. This research was supported in part by the Intramural Research Program of the National Human Genome Research Institute and the National Heart, Lung, and Blood Institute (NIH) and by NIH Grant HL-18645 (to T.N.W.). M.E. was supported by grants from the Tore Nilsson Foundation, the Åke Wiberg Foundation, the Hagelen Foundation, the Loo and Hans Osterman Foundation, the Torsten and Ragnar Söderberg Foundation, the Jeansson Foundation, the Swedish Research Council, and the Swedish Foundation for Strategic Research.

1. DeBusk, F. L. (1972) *J. Pediatr. (Berlin)* **80,** 697–724.
2. Baker, P. B., Baba, N. & Boesel, C. P. (1981) *Arch. Pathol. Lab. Med.* **105,** 384–386.
3. Stehbens, W. E., Wakefield, S. J., Gilbert-Barness, E., Olson, R. E. & Ackerman, J. (1999) *Cardiovasc. Pathol.* **8,** 29–39.
4. Stehbens, W. E., Delahunt, B., Shozawa, T. & Gilbert-Barness, E. (2001) *Cardiovasc. Pathol.* **10,** 133–136.
5. Ackerman, J. & Gilbert-Barness, E. (2002) *Pediatr. Pathol. Mol. Med.* **21,** 1–13.
6. Eriksson, M., Brown, W. T., Gordon, L. B., Glynn, M. W., Singer, J., Scott, L., Erdos, M. R., Robbins, C. M., Moses, T. Y., Berglund, P., *et al.* (2003) *Nature* **423,** 293–298.
7. De Sandre-Giovannoli, A., Bernard, R., Cau, P., Navarro, C., Amiel, J., Boccaccio, I., Lyonnet, S., Stewart, C. L., Munnich, A., Le Merrer, M., *et al.* (2003) *Science* **300,** 2055.
8. Bonne, G. & Levy, N. (2003) *Lancet* **362,** 1585–1586; author reply, 1586.
9. Csoka, A. B., Cao, H., Sammak, P. J., Constantinescu, D., Schatten, G. P. & Hegele, R. A. (2004) *J. Med. Genet.* **41,** 304–308.
10. Fukuchi, K., Katsuya, T., Sugimoto, K., Kuremura, M., Kim, H. D., Li, L. & Ogihara, T. (2004) *J. Med. Genet.* **41,** e67.
11. Plasilova, M., Chattopadhyay, C., Pal, P., Schaub, N. A., Buechner, S. A., Mueller, H., Miny, P., Ghosh, A. & Heinimann, K. (2004) *J. Med. Genet.* **41,** 609–614.
12. Huang, S., Kennedy, B. K. & Oshima, J. (2005) *Novartis Found. Symp.* **264,** 197–202; discussion 202-207, 227–230.
13. Gruenbaum, Y., Margalit, A., Goldman, R. D., Shumaker, D. K. & Wilson, K. L. (2005) *Nat. Rev. Mol. Cell Biol.* **6,** 21–31.
14. Goldman, R. D., Gruenbaum, Y., Moir, R. D., Shumaker, D. K. & Spann, T. P. (2002) *Genes Dev.* **16,** 533–547.
15. Capell, B. C., Erdos, M. R., Madigan, J. P., Fiordalisi, J. J., Varga, R., Conneely, K. N., Gordon, L. B., Der, C. J., Cox, A. D. & Collins, F. S. (2005) *Proc. Natl. Acad. Sci. USA* **102,** 12879–12884.
16. Agarwal, A. K., Fryns, J. P., Auchus, R. J. & Garg, A. (2003) *Hum. Mol. Genet.* **12,** 1995–2001.
17. Sullivan, T., Escalante-Alcalde, D., Bhatt, H., Anver, M., Bhat, N., Nagashima, K., Stewart, C. L. & Burke, B. (1999) *J. Cell Biol.* **147,** 913–920.
18. Mounkes, L. C., Kozlov, S., Hernandez, L., Sullivan, T. & Stewart, C. L. (2003) *Nature* **423,** 298–301.
19. Yang, S. H., Bergo, M. O., Toth, J. I., Qiao, X., Hu, Y., Sandoval, S., Meta, M., Bendale, P., Gelb, M. H., Young, S. G., *et al.* (2005) *Proc. Natl. Acad. Sci. USA* **102,** 10291–10296.
20. Lee, E. C., Yu, D., Martinez de Velasco, J., Tessarollo, L., Swing, D. A., Court, D. L., Jenkins, N. A. & Copeland, N. G. (2001) *Genomics* **73,** 56–65.
21. Schildmeyer, L. A., Braun, R., Taffet, G., Debiasi, M., Burns, A. E., Bradley, A. & Schwartz, R. J. (2000) *FASEB J.* **14,** 2213–2220.
22. Lammerding, J., Schulze, P. C., Takahashi, T., Kozlov, S., Sullivan, T., Kamm, R. D., Stewart, C. L. & Lee, R. T. (2004) *J. Clin. Invest.* **113,** 370–378.
23. Glynn, M. W. & Glover, T. W. (2005) *Hum. Mol. Genet.* **14,** 2959–2969.
24. Young, S. G., Fong, L. G. & Michaelis, S. (2005) *J. Lipid Res.* **46,** 2531–2558.
25. Toth, J. I., Yang, S. H., Qiao, X., Beigneux, A. P., Gelb, M. H., Moulson, C. L., Miner, J. H., Young, S. G. & Fong, L. G. (2005) *Proc. Natl. Acad. Sci. USA* **102,** 12873–12878.
26. Horwitz, E. M., Gordon, P. L., Koo, W. K., Marx, J. C., Neel, M. D., McNall, R. Y., Muul, L. & Hofmann, T. (2002) *Proc. Natl. Acad. Sci. USA* **99,** 8932–8937.
27. Liu, P., Jenkins, N. A. & Copeland, N. G. (2003) *Genome Res.* **13,** 476–484.
28. Schmidt, R. and. Wirtala, J. (1996) *J. Histotechnol.* **19,** 325–327.
29. Farb, A., Weber, D. K., Kolodgie, F. D., Burke, A. P. & Virmani, R. (2002) *Circulation* **105,** 2974–2980.
30. Lara, S. L., Evanko, S. P. & Wight, T. N. (2001) *Methods Mol. Biol.* **171,** 271–290.